Comparison of soft magnetic properties of $Ni_{81}Fe_{19}$ film with different substrates used for microfluxgate

Yang Shanglin, Liu Shibin, Guo Bo, Feng Wenguang, Hou Xiaowei

School of Electronics and Information, Northwestern Polytechnical University, Xi'an, People's Republic of China
E-mail: liushibin@nwpu.edu.cn

Published in Micro & Nano Letters; Received on 25th April 2013; Revised on 19th June 2013; Accepted on 2nd July 2013

The soft magnetic properties of $Ni_{81}Fe_{19}$ films, respectively, composed of Ti, Ta and Cr substrates used for a microfluxgate have been studied in this reported work. The films were characterised using a transmission electron microscope, X-ray diffraction, a vibrating sample magnetometer and a fluxgate solenoid. The testing results showed that Ta substrate film, because of its ladder rising hysteresis loop, is the most appropriate one for the fluxgate core in these four kinds of $Ni_{81}Fe_{19}$ films, the original $Ni_{81}Fe_{19}$ film, and the film with Ti substrate takes second place, and the Cr substrate film would not be suitable as the fluxgate core because of its bad soft magnetic properties.

1. Introduction: The fluxgate sensor is a weak magnetic field measurement sensor with good performances [1], and is widely used in industry, military, aerospace and life consumption fields. Owing to its advantages of small size and easy integration, a microfluxgate has been extensively studied. In a fluxgate structure, the soft magnetic property of the core directly determines the performance of the fluxgate. There are general requirements for the magnetic core material of a fluxgate sensor, such as high permeability and low coercivity, magnetostriction, saturation magnetisation and internal stress [2]. Compared with ferrite, silicon steel and amorphous alloy thin film, $Ni_{81}Fe_{19}$ film has good soft magnetic properties and processing compatibility concurrently, hence it is the preferred material for a microfluxgate sensor. Using micro/nanotechnology to fabricate the microfluxgate, it is necessary to sputter a substrate to increase the adhesion force between the $Ni_{81}Fe_{19}$ film and the silicon substrate, however the most common substrate materials such as Ti, Ta and Cr [3] affect the soft magnetic properties of $Ni_{81}Fe_{19}$, and some further research needs to be done on this issue.

Li *et al*. [4] had investigated the magnetic properties of Ti/$Ni_{81}Fe_{19}$ film, and pointed out that interdiffusion and climination of stress may result in variation of properties; Yu *et al*. [5] thought a Ti seed layer could induce a strong (111) texture in the bottom of the Co/NiFe bilayer, and domain wall mobility was higher because of the strong crystallographic texture and large grain size in the bilayer; Mao *et al*. [6] had deposited Ta/NiFe films, respectively, using ion beam deposition, pulse, static magnetron sputtering and indicated that high quality crystallisation is the reason for the excellent magnetic properties; Nakatani *et al*. [7] had investigated the magnetoresistance effects and film structures in (Fe-Mn/Ni-Fe/Cu/Ni-Fe/buffer/Si) sandwiches with various substrate layer materials, and found that a Nb, Ta, Ti, Zr or Hf substrate layer can cause strong (111) texture, which Cu, Ag, Au and Cr cannot; Choe and Steinback [8] had investigated the surface roughness effect on the magnetic properties of Ta/NiFe, and found in a wide range of thicknesses NiFe (111) smooth substrate could yield higher anisotropy and lower coercivity; Sharp and Archibald [9] had made multilayer Cr/NiFe films, and reported that because of exchange anisotropy between antiferromagnetic material (Cr) and ferromagnetic material (NiFe), crystal anisotropy, magnetostriction and so on are not unidirectional; Dreyer *et al*. [10] had prepared spin-polarised tunnelling on the terraces of antiferromagnetic Cr (001), and found that monolayer thick permalloy exhibited pyramidal islands oriented along the Cr (100) direction; Lee *et al*. [11] had used a thin $(Ni_{0.81}Fe_{0.19})_{1-x}Cr_x$ seed layer and obtained high anisotropic magnetoresistivity in $Ni_{81}Fe_{19}$ film, and found that the NiFeCr seed layer caused the formation of large (111) textured gains in NiFe and the interface between those two layers was quite smooth.

To improve the soft magnetic properties of the magnetic core, we chose $Ni_{81}Fe_{19}$ whose magnetostriction constant λ_{111} is zero, so as to obtain minimum noise [2]. According to the theory of magnetic material, material permeability and coercive force depends on the crystal anisotropy constant, internal stress and magnetostriction constant. In this reported work, we studied the soft magnetic properties of $Ni_{81}Fe_{19}$ film with Ti, Ta and Cr substrates. We first sputtered a metal substrate layer (Ti, Ta or Cr) using magnetron sputtering apparatus on the Si (111) substrate, then sputtered $Ni_{81}Fe_{19}$ on the base temperature of 400°C. We used a transmission electron microscope (TEM), X-ray diffraction (XRD), a vibrating sample magnetometer (VSM) and fluxgate solenoid, respectively, for the prepared sample films for microstructure observation, crystal orientation, hysteresis loop measurement and fluxgate signal, and found that Ta substrate of $Ni_{81}Fe_{19}$ film is most suitable for the fluxgate core, the original $Ni_{81}Fe_{19}$ film and Ti substrate film were the second degree and the Cr substrate of the film is not suitable for the fluxgate core.

2. Experiment and test: The experimental fluxgate core films were prepared by JPG450 magnetron sputtering apparatus made by the Shenyang Scientific Instruments plant of the Chinese Academy of Sciences. In the production process of the four kinds of samples, the specification of 30 × 1.5 mm Si (111) tablets were cleaned by 5 min ultrasonic for removing surface organic impurities, then dried by nitrogen and fixed in the chamber of the sputtering apparatus. Under the condition of 5.0×10^{-4} Pa base pressure, the standard condition per minute (SCCM) 15 ml argon, 1.5 Pa sputtering pressure, 90 W DC sputtering power, 100 V bias voltage, 99.99% Ti, 99.99% Ta and 99.8% Cr target materials, sputtered 3 min to deposit substrate layer films. Then, at the base pressure of 5.0×10^{-4} Pa, the base temperature of 400°C, argon flow for 40 SCCM, 3.0 Pa sputtering pressure, 160 W radiofrequency (RF) power, 13.56 MHz RF frequency, 99.99% $Ni_{81}Fe_{19}$ target material, sputtered for 2 h to form $Ni_{81}Fe_{19}$ thin layer.

The thickness of each layer in the four films had been measured using a Bruker Dektak XT stylelus profiler, and we used TEM to observe the film surface condition and energy diffraction spectrum (EDS) in magnifications of 10 000, 50 000 and 100 000, respectively. The crystal structures of the four films were analysed by XRD in

© The Institution of Engineering and Technology 2013

doi: 10.1049/mnl.2013.0230

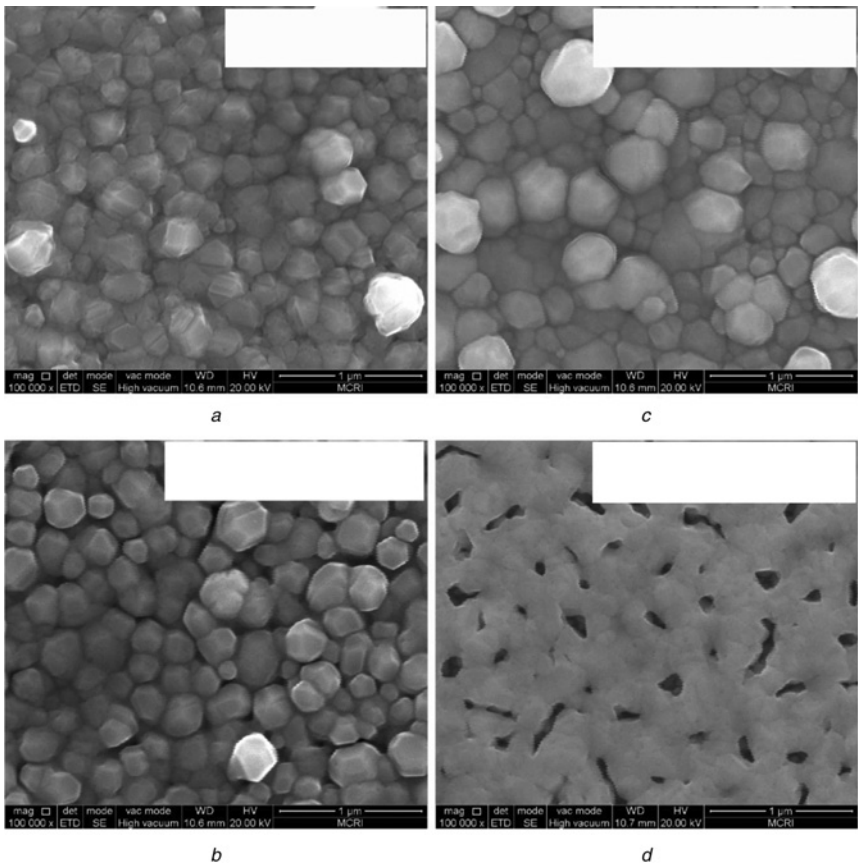


Figure 1 *TEM diagram of four film samples*
a $Ni_{81}Fe_{19}$
b $Ni_{81}Fe_{19}$/Ti
c $Ni_{81}Fe_{19}$/Ta
d $Ni_{81}Fe_{19}$/Cr

the diffraction angle of 15–100°. The room temperature magnetic hysteresis of the four films had also been tested.

3. Experimental results and analysis

3.1. Surface morphology: The thickness of each layer in the sample films are Ti 45 nm, Ta 46 nm, Cr 69 nm and $Ni_{81}Fe_{19}$ 500 nm, respectively. Fig. 1 and Table 1 show the surface morphology and composition of the four films separately. Fig. 1 shows that the original $Ni_{81}Fe_{19}$ film, Ti and Ta substrate presented the granular crystal where the particles on the surface were bigger than the ones inside; however, the $Ni_{81}Fe_{19}$ film with Cr substrate are bound into blocks on the surface, thus it is hard to distinguish the crystal particles.

From Table 1 we can see that although the surface composition of the original $Ni_{81}Fe_{19}$ film, Ti and Ta substrate had a small amount of C and Si elements besides the Fe and Ni elements, the surface composition of the $Ni_{81}Fe_{19}$ film with Cr substrate not only contained Fe and Ni elements, but also a Cr element. The surface had a Si element because the basement Si tablets are not fully covered by film, and the reason why C element existed was perhaps because of organic pollution which had been absorbed to the sample surface in the testing condition.

Table 1 EDS of four film samples in element weight percentage

	Elements						
Films	C	Si	Fe	Ni	Ti	Ta	Cr
$Ni_{81}Fe_{19}$	4.54	4.68	17.17	84.20	0	0	0
$Ni_{81}Fe_{19}$/Ti	4.46	5.02	17.65	82.91	0	0	0
$Ni_{81}Fe_{19}$/Ta	6.54	5.71	17.75	82.96	0	0	0
$Ni_{81}Fe_{19}$/Cr	2.52	4.07	17.50	83.04	0	0	3.26

Fig. 1 and Table 1 show remarkable differences between the $Ni_{81}Fe_{19}$ film with Cr substrate and the other three kinds of films, the reasons causing this condition may be the interpenetration of Cr and $Ni_{81}Fe_{19}$ which formed a new NiFeCr film.

3.2. Crystal structure: Four XRD charts of sample films are shown in Fig. 2 in which there is only a little difference. The four films are polycrystalline, in which the (111) peak was the highest, the (200) peak took second place, however the original $Ni_{81}Fe_{19}$ film had a lower strength ratio of (111) peak to (200) peak compared with the other films. Owing to the containing of the Cr element, the diffraction peak of the Cr substrate film was probably the NiFeCr peak. We know that $\lambda_{111} = 0$ in Ni content near 80%, hence the (111) crystal peak is helpful for increasing the properties of soft magnetic materials. Using the Scherrer formula to calculate average grain size the four film grain sizes are as follows: the original $Ni_{81}Fe_{19}$ film 20 nm, Ti substrate 22 nm, Ta substrate 21 nm and Cr substrate 28 nm. In soft magnetic thin film materials, the coercive force (H_c) follows the power law index dependence grain size D [12]. The smaller D makes smaller coercive force and better performance of soft magnetic properties.

3.3. Soft magnetic properties: Fig. 3 are the magnetic hysteresis diagrams of these four kinds of thin films, from which we can see the results are consistent with the results in the former Section; the coercive force of the four sample films increased followed by

© The Institution of Engineering and Technology 2013

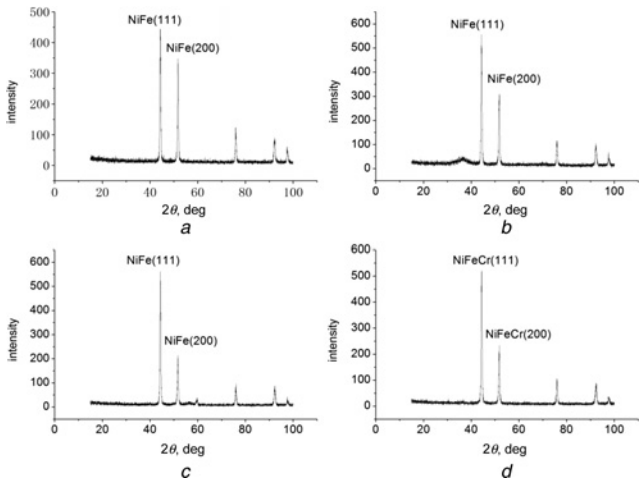


Figure 2 *XRD chart of four film samples*
a $Ni_{81}Fe_{19}$
b $Ni_{81}Fe_{19}$/Ti
c $Ni_{81}Fe_{19}$/Ta
d $Ni_{81}Fe_{19}$/Cr

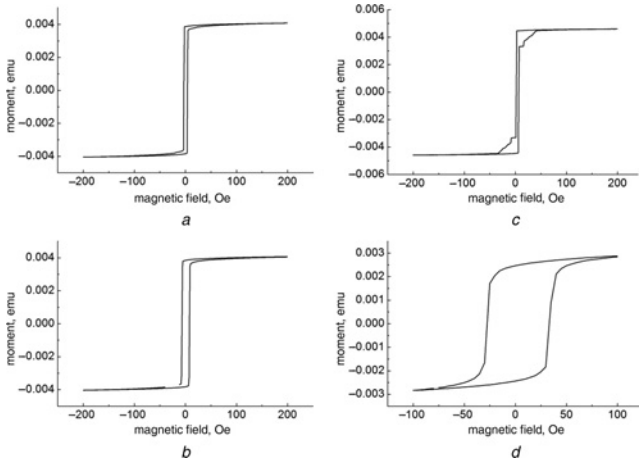


Figure 3 *VSM curve of four film samples*
a $Ni_{81}Fe_{19}$
b $Ni_{81}Fe_{19}$/Ti
c $Ni_{81}Fe_{19}$/Ta
d $Ni_{81}Fe_{19}$/Cr

$H_{cNi_{81}Fe_{19}} < H_{cNi_{81}Fe_{19}/Ta} < H_{cNi_{81}Fe_{19}/Ti} < H_{cNi_{81}Fe_{19}/Cr}$, of which the original $Ni_{81}Fe_{19}$ film, Ti substrate and Ta substrate thin film had smaller coercive force, but the coercive force of the Cr substrate thin film was greatly increased, and the saturated magnetic induction intensity B_s relationship were $B_{sNi_{81}Fe_{19}/Cr} < B_{sNi_{81}Fe_{19}} = B_{sNi_{81}Fe_{19}/Ti} < B_{sNi_{81}Fe_{19}/Ta}$. The reason that caused the Cr substrate film $B_{sNi_{81}Fe_{19}/Cr}$ to decrease may be that the Cr element had interfused in the $Ni_{81}Fe_{19}$ film. From Fig. 3 we can see that the $Ni_{81}Fe_{19}$/Ta film magnetic hysteresis loop presented a strange change, which in low magnetic induction intensity B appeared as nonlinear inflection point and it changed very steeply, and this characteristic is just what the fluxgate sensor core needed, because the same magnetic permeability and low magnetic induction intensity would be corresponding to the small magnetic field intensity, which can further reduce fluxgate power consumption, and a steep permeability change also increases the sensitivity of the sensor output. At the same time, because it has a small coercive force, the Ta substrate film had a low hysteresis loss. The reason why this magnetic hysteresis loop appeared may be that the exchange coupling effect had taken place between the Ta substrate and $Ni_{81}Fe_{19}$ films, which resulted in the magnetic hysteresis appearing in symmetry steps around the zero field.

3.4. Fluxgate signal: In this work we inserted four different substrate core samples into the fluxgate solenoid, respectively, which consists of two identical solenoids. Each solenoid is made of 326 primary and 1150 secondary coils, which wound on the 30 mm-long skeleton. Two coils are embedded into the cube frame to ensure that the two solenoids are parallel. Then, it connects two primary coils and two secondary coils, and ensures that they work in a magnetic fluxgate way.

According to Liu [13], the optimal excitation current i_{mo} is defined as: excited under the sinusoidal wave, i_{mo} is the excitation current root mean square (RMS) which makes the second harmonic amplitude of measuring coil output voltage reach maximum. Excited under a 132 kHz sinusoidal wave, with various measured magnetic fields from 0 to 70 A/m, the optimum excitation current i_{mo} and the output voltage second harmonic amplitude U_{2m} of four different substrate film cores were measured. Owing to the bad magnetic property of the Cr substrate $Ni_{81}Fe_{19}$ film core compared with the other three substrate film cores, whose fluxgate signal is hard to obtain, hence, the Cr substrate film core is no longer to be discussed in this Letter. The test results of the other three samples are shown in Figs. 4 and 5. From Fig. 4, we can see that under different measured magnetic field Ta substrate, film core of $Ni_{81}Fe_{19}$ films had minimum t_{mo}, the original $Ni_{81}Fe_{19}$ film followed, and the Ti substrate's t_{mo} is largest, this is because the Ta substrate film core hysteresis loop under small magnetic fields appears as a nonlinear inflection point, this result being

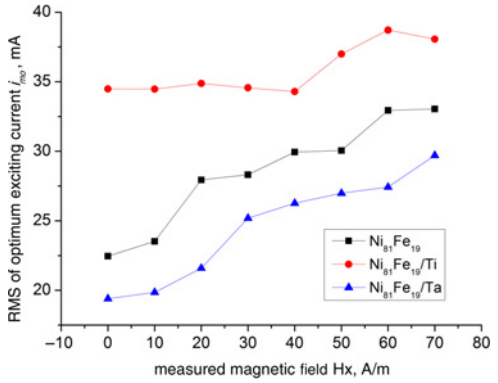


Figure 4 *RMS of optimum exciting Current i_{mo} against measured magnetic field H_X*

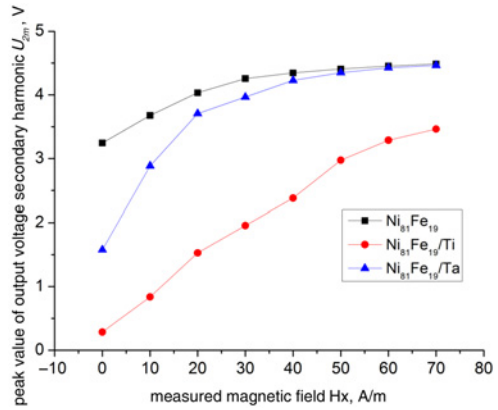


Figure 5 *Peak value of output voltage secondary harmonic U_{2m} against measured magnetic field H_X*

© The Institution of Engineering and Technology 2013

doi: 10.1049/mnl.2013.0230

consistent with the former analysis of the hysteresis loop. Meanwhile, under the same exciting current, from Fig. 5 we can see that the original $Ni_{81}Fe_{19}$ film had the largest U_{2m} under the measured magnetic field from 0 to 70 A/m, the Ta substrate had subprime U_{2m} which was less than the original $Ni_{81}Fe_{19}$ film, whereas the Ti substrate film had much smaller U_{2m} than the first two, however its output linearity was higher. The results agreed with our former analysis of hysteresis loops, in which the Ti substrate film had greater coercivity and a slower rate of magnetic hysteresis loop. We can also see from Fig. 5 that the Ta substrate and the original $Ni_{81}Fe_{19}$ film had a big zero offset, the reason may be that the two samples themselves contain large noise.

4. Conclusion: Four kinds of $Ni_{81}Fe_{19}$ film separately with Ti substrate, Ta substrate and Cr substrate and the original $Ni_{81}Fe_{19}$ film had been prepared by magnetron sputtering apparatus, then we used TEM, XRD and VSM to test the surface morphology, crystal structure and hysteresis loop of these four films, respectively. Finally, we formed the following conclusions:

1. In the TEM diagram, the original $Ni_{81}Fe_{19}$ film, Ti and Ta substrate presented the granular crystal, but Cr substrate $Ni_{81}Fe_{19}$ film is bound to block, therefore it is difficult to distinguish grain. Besides, we can see that Cr substrate $Ni_{81}Fe_{19}$ film had been infiltrated by the Cr element from EDS data.
2. From the XRD chart, we can see that the four films are polycrystalline, in which the (111) peak was the highest, the (200) peak takes second place. Through the Scherrer formula, we can find out that the grain size of the original $Ni_{81}Fe_{19}$ film was the minimum, and Cr substrate film maximum.
3. The VSM chart showed that the magnetic hysteresis of the original $Ni_{81}Fe_{19}$ film, Ni and Ta substrate $Ni_{81}Fe_{19}$ film had the smaller coercive force, but the Cr substrate thin film had a greater coercive force; when the magnetic induction intensity is about 0.003 emu, there appears a step in the rising phase in the hysteresis loop of Ta substrate film, the same phenomenon also comes up at −0.003 emu in the descent phase. These characteristics, which can reduce power consumption and improve the sensitivity of fluxgate, just meets the requirements of fluxgate.
4. The fluxgate signal revealed that the Ta substrate film had the smallest exciting current and relatively larger second harmonic amplitude of output voltage in those four fluxgate systems with different film cores, which was consistent with the VSM results; however the Cr substrate film had no fluxgate signal in very large exciting current.
5. Comprehensively considering the above, in these four kinds of $Ni_{81}Fe_{19}$ films, Ta substrate film is more appropriate for the fluxgate core, the original $Ni_{81}Fe_{19}$ film and Ti substrate film come second and Cr substrate film would not be suitable as fluxgate core material.

5. Acknowledgments: This study is supported by the National Natural Science Foundation of China (grant no. 60874101), the Higher School Specialised Research Fund for the Doctoral Program of 2012 (grant no. 20126102110031) and the 2013's Graduate Students Entrepreneurial Seed Fund of Northwest Polytechnical University (grant nos Z2013074 and Z2013075).

6 References

[1] Ripka P., Billingsley S.W.: 'Fluxgate: tuned vs. untuned output', *IEEE Trans. Magn.*, 1998, **34**, (4), pp. 1303–1305
[2] Ripka P.: 'Magnetic sensors and magnetometers' (Artech House, 2001)
[3] Gad-el-Hak M.: 'MEMS design and fabrication' (Mechanical Industry Press, 2010)
[4] Li S.X., Yan M.L., Yu C.T., Lai W.Y.: 'Effect of interface on the properties of Ti/NiFe thin-films', *J. Appl. Phys.*, 1994, **75**, (10), pp. 6504–6506
[5] Yu A.C.C., Petford-Long A.K., O'Grady K., Miyazaki T.: 'Effect of Ti seed layer on the magnetization reversal process of Co/NiFe/Al-oxide/NiFe junction films', *J. Appl. Phys.*, 2002, **91**, (8), pp. 5234–5239
[6] Mao M., Leng Q., Huai Y., *ET AL.*: 'Characterization of ion beam and magnetron sputtered thin Ta/NiFe films', *J. Appl. Phys.*, 1999, **85**, (8), pp. 5780–5782
[7] Nakatani R., Hoshino K., Noguchi S., Sugita Y.: 'Magnetoresistance and preferred orientation in Fe-Mn/Ni-Fe/Cu/Ni-Fe sandwiches with various buffer layer materials', *Jpn. J. Appl. Phys.*, 1994, **33**, (Part 1), pp. 133–137
[8] Choe G., Steinback M.: 'Surface roughness effects on magnetoresistive and magnetic properties of NiFe thin films', *J. Appl. Phys.*, 1999, **85**, (8), pp. 5777–5779
[9] Sharp R.W., Archibald P.C.: 'Unidirectional anisotropy in multilayer films of Cr and NiFe', *J. Appl. Phys.*, 1966, **37**, (3), pp. 1462–4
[10] Dreyer M., Lee J., Krafft C., Gomez R.: '(Towards) spin-polarized scanning tunneling microscopy of NiFe films on a chromium(001) single crystal: growth and electronic structure of permalloy', *J. Appl. Phys.*, 2005, **97**, (10), p. 10E703
[11] Lee W., Toney M., Mauri D.: 'High magnetoresistance in sputtered permalloy thin films through growth on seed layers of $(Ni_{0.81}Fe_{0.19})_{1-x}Cr_x$', *IEEE Trans. Magn.*, 2000, **36**, (1), pp. 381–385
[12] Liu Y., Sellmyer D.J., Shindo D.: 'Handbook of advanced magnetic materials: Vol 1. Nanostructural effects' (Springer, 2005)
[13] Liu S.: 'Research on micro intelligent magnetic heading system', Northwestern Polytechnical University, Xi'an, 2001, pp. 13–32

© The Institution of Engineering and Technology 2013